

IRE1 α is critical for Kaempferol-induced neuroblastoma differentiation

Ahmad Abdullah¹, Priti Talwar¹, Christian Lefebvre d'Hellencourt² and Palaniyandi Ravanan¹

¹ Apoptosis and Cell Survival Research Lab, Department of Biosciences, School of Biosciences and Technology, VIT University, Vellore, India

² Institut National de la Santé et de la Recherche Médicale, UMR Diabète Athérombose Thérapies Réunion Océan Indien, Université de La Réunion, Saint-Denis de La Réunion, France

Keywords

IRE1 α ; kaempferol; neuroblastoma; neuronal differentiation; XBP1

Correspondence

P. Ravanan, Department of Biosciences, School of Biosciences and Technology, VIT University, Vellore, Tamil Nadu 632014, India

Tel: +91 9842063012

E-mail: ravanan.p@vit.ac.in

(Received 12 October 2018, revised 13 January 2019, accepted 31 January 2019)

doi:10.1111/febs.14776

Neuroblastoma is an embryonic malignancy that arises out of the neural crest cells of the sympathetic nervous system. It is the most common childhood tumor known for its spontaneous regression via the process of differentiation. The induction of differentiation using small molecules such as retinoic acid is one of the therapeutic strategies to treat the residual disease. In this study, we have reported the effect of kaempferol (KFL) in inducing differentiation of neuroblastoma cells *in vitro*. Treatment of neuroblastoma cells with KFL reduced the proliferation and enhanced apoptosis along with the induction of neuritogenesis. Analysis of the expression of neuron-specific markers such as β -III tubulin, neuron-specific enolase, and *N-myc* downregulated gene 1 revealed the process of differentiation accompanying KFL-induced apoptosis. Further analysis to understand the molecular mechanism of action showed that the effect of KFL is mediated by the activation of the endoribonuclease activity of inositol-requiring enzyme 1 alpha (IRE1 α), an endoplasmic reticulum-resident transmembrane protein. *In silico* docking analysis and biochemical assays using recombinant human IRE1 α confirm the binding of KFL to the ATP-binding site of IRE1 α , which thereby activates IRE1 α ribonuclease activity. Treatment of cells with the small molecule STF083010, which specifically targets and inhibits the endoribonuclease activity of IRE1 α , showed reduced expression of neuron-specific markers and curtailed neuritogenesis. The knockdown of IRE1 α using plasmid-based shRNA lentiviral particles also showed diminished changes in the morphology of the cells upon KFL treatment. Thus, our study suggests that KFL induces differentiation of neuroblastoma cells via the IRE1 α -XBP1 pathway.

Introduction

Neuroblastoma, the most common solid extra cranial malignant tumor of infants originates from the precursor cells that derived from the neural crest tissues [1].

These cells can get differentiated into any other cell types of neural origin [2]. The clinical representation of the disease varies drastically from a mass with no

Abbreviations

ATRA, all-trans retinoic acid; DNAJC, DnaJ homolog subfamily C; DR5, death receptor 5; ERDJ, endoplasmic reticulum DnaJ; ER, endoplasmic reticulum; IRE1 α , inositol-requiring enzyme 1 alpha; MAPK, mitogen-associated protein kinase; MTT, 3-[4,5 dimethylthiazol - 2 -yl] - 2,5 -diphenyltetrazolium bromide; NDRG, N-myc downregulated gene; NSE, neuron-specific enolase; PDIA, protein disulphide isomerase A; TNFR1, tumor necrosis factor receptor 1; XBP1, X-box-binding protein 1.

symptoms to a primary tumor causing critical illness with tumor disseminates into the neck, thorax, abdomen, or pelvis and stands as the most commonly diagnosed tumor in early childhood [3]. The heterogeneity of neuroblastoma tumors makes intense chemoradiotherapy as a therapeutic intervention. Therefore, for minimizing the effect of chemoradiotherapy, alternative therapeutic strategies targeting crucial proteins involved in the tumor progression are needed. The derivatives of retinoic acid (RA) are widely used clinically after cytotoxic therapy as differentiation inducing agents for controlling minimal residual disease in high-risk neuroblastoma patients [4].

Retinoic acid, a derivative of vitamin A has been shown to promote differentiation of embryonic, neural, and mesenchymal stem cells [5]. All-*trans* RA (ATRA), 9-*cis* RA, and 13-*cis* RA are the well-known RA isomers that have been shown to induce differentiation and used in the treatment of neuroblastoma [6]. Resistance to RA therapy is commonly observed *in vitro* as well as clinically, due to the mutations in RA receptor (RAR) gene or RAR receptor [7]. In addition, trichostatin A, kenpaullone, and SB-216763 has also been reported to induce neuritogenesis *in vitro* [8,9]. Recent studies reported alectinib (Anaplastic Lymphoma Kinase inhibitor) and YK-4-279 (mitosis disruptor) as promising candidates for neuroblastoma treatment by emphasizing the lack of effective therapies at present in clinics [10,11]. Inositol-requiring enzyme 1 alpha (IRE1 α) is an endoplasmic reticulum (ER)-resident protein involved in the unfolded protein response (UPR) pathway. It has a luminal N-terminal domain inside ER lumen and two functional enzymatic cytoplasmic domains having kinase and endoribonuclease activities. The activation of IRE1 α is via the accumulation of misfolded proteins or by other physiological stimuli not limiting to lipid perturbation, viral infection, or immune response [12] which leads to the initiation of its kinase or endoribonuclease activity. The kinase activity is known for the recruitment of TRAF2 protein and activation of c-Jun N-terminal kinase (JNK)-mediated signaling cascade, thereby driving cells toward an apoptotic response [13]. The ribonuclease activity of IRE1 α can cleave multiple RNA substrates involved in diverse cell response pathways with X-box binding protein 1 (*Xbp1*) mRNA being the major substrate. A spliced form of *Xbp1* mRNA gets translated into an active transcription factor XBP1s that is involved in the transcription of variety of genes [14]. The mouse embryos lacking IRE1 α died after 11.5–14.5 days post-coitum emphasizing the role of IRE1 α in the developmental stages of the organism [15]. Moreover,

the IRE1 α -XBP1 pathway of gene activation is known to be a critical factor involved in the differentiation of plasma cells, osteoblasts, and adipocytes [16–18].

Kaempferol (KFL) is a phytoestrogen that belongs to the class of flavonoids and is known to exhibit antioxidant, anti-inflammatory, and anticancer activities [19]. In our attempt toward identifying an inhibitor against ER stress-induced cell death, we found KFL to rescue mammalian cells from apoptosis induced by multiple cell death inducers by acting as an allosteric inhibitor for executioner caspases [20]. While performing the experiments we observed changes in morphology of IMR32 cells, a human neuroblastoma cell line with neurite like outgrowths, upon prolong incubation in the presence of KFL.

In this study, we have investigated the effect of KFL on neuroblastoma cell lines, IMR32 and Neuro2a. Observations made in our experiments suggest that KFL-mediated differentiation of neuroblastoma cells happens via the activation of IRE1 α endoribonuclease activity. Since KFL is a dietary polyphenol and cohort studies had been performed for understanding its effect on various other cancers [21], it could also be explored for its effect on neuroblastoma in preclinical and clinical trials.

Results

Kaempferol induces neuroblastoma differentiation and decreases cell viability

To understand the effect of KFL on neuroblastoma cells, we employed IMR32 and Neuro2a cell lines, well-established *in vitro* models that have been used widely for understanding neuroblastoma differentiation. IMR32 and Neuro2a cells were incubated in the presence of KFL (50 μ M) for 4 days; cells cultured in the presence of ATRA (25 μ M) that served as a positive control. After 48 h of incubation, we observed morphological changes including neurite outgrowth associated with decreased proliferation and viability. To confirm whether the neurite outgrowth is due to cellular differentiation, we performed immunocytochemistry to analyze the expression of β -III tubulin, a neuronal differentiation marker. The significant increase in the expression level of β -III tubulin in the KFL- and ATRA-treated cells compared to the controls confirmed the neurite outgrowth to be due to the cellular differentiation (Fig. 1A). A further assessment on the viability of the cells using 3-[4,5-dimethylthiazol-2-yl]-2,5-diphenyltetrazolium bromide (MTT) assay and trypan blue dye exclusion assay revealed that KFL decreased the viability of

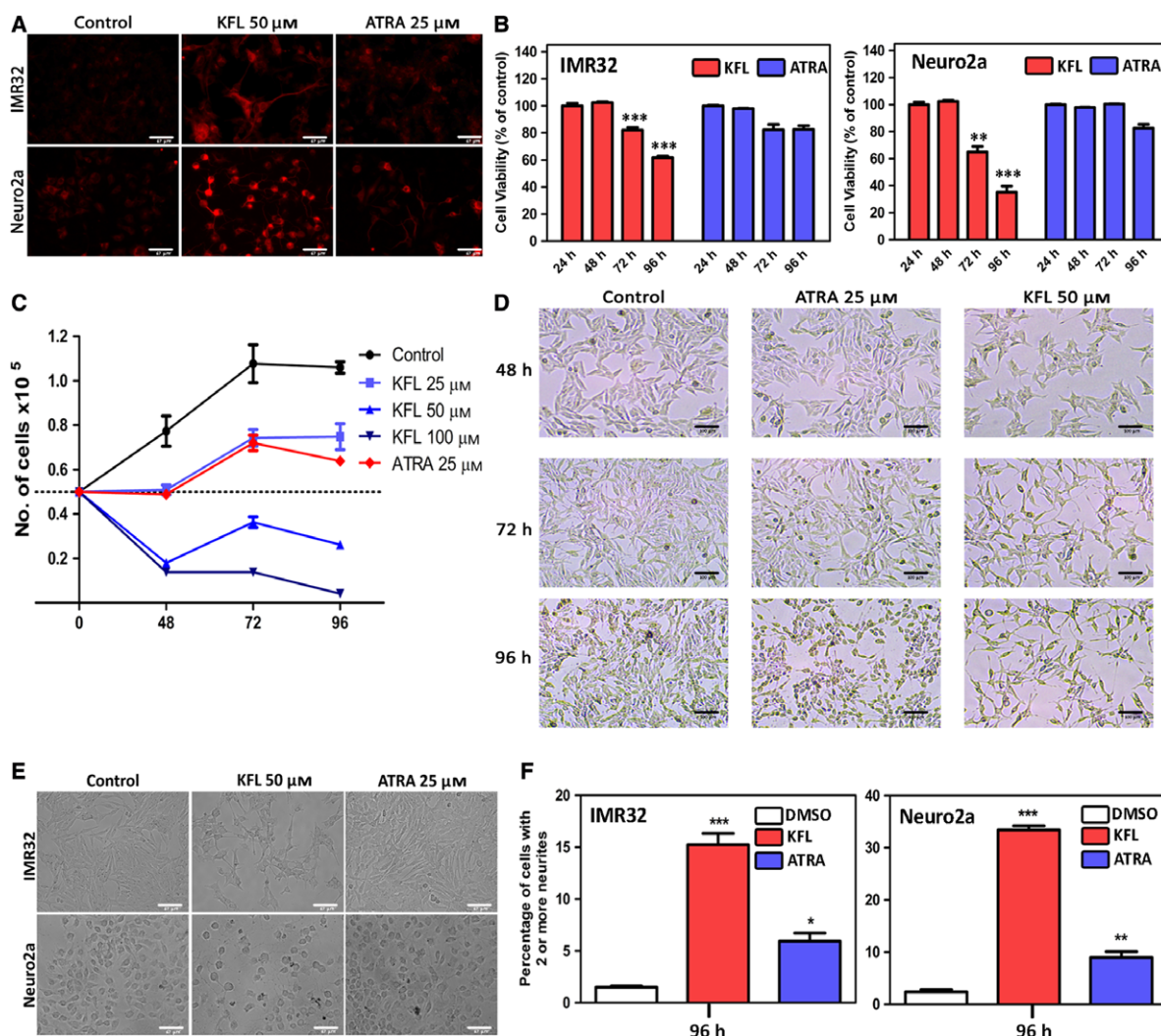


Fig. 1. KFL induced differentiation in neuroblastoma cells. (A) IMR32 and Neuro2a cells were seeded in 12-well plate (50×10^3 cells per well) and treated with KFL or ATRA to induce differentiation. After 96 h of incubation, immunocytochemistry was performed to observe the increase in the expression of β III tubulin (red), a neuron-specific marker protein. Representative images of experiments performed for three times. Scale bars = 67 μ m. (B) IMR32 and Neuro2a cells were treated with KFL (50 μ M) or ATRA (25 μ M) and assayed for cell death using MTT assay. The x-axis denotes time point in hours (24, 48, 72, 96 h) and y-axis shows the relative cell survival compared to DMSO-treated control cells. The assay was performed in triplicate and the graph represents the average \pm SEM from three independent experiments performed. (** $P < 0.01$; *** $P < 0.001$; two-way ANOVA). (C) Trypan blue dye exclusion assay was performed to analyze the effect of KFL and ATRA on the proliferation of IMR32 cells. In a 24-well plate, 50×10^3 were seeded on day 0 and treated with respective concentrations of KFL or ATRA. DMSO-treated cells served as control. Cells were collected on day 2, day 3, and day 4 and stained using trypan blue dye, and then live cells were counted manually using haemocytometer. Data represented as average \pm SEM of counting obtained from three independent experiments performed in triplicates (*** $P < 0.001$; two-way ANOVA). Dashed line represents the seeding density of 50×10^3 cells on day 0. (D) IMR32 cells (seeding density at 10×10^4 cells per 60 mm dish) treated with ATRA and KFL were viewed under phase contrast microscope equipped with color camera at 48, 72, and 96 h time points. Percent DMSO-treated cells were represented as control. Images showed a reduction in confluence and change in morphology in KFL 50 μ M and ATRA 25 μ M treated cells compared to the control cells. Representative image of experiments performed for three times. Scale bars = 100 μ m. (E) Change in the morphology of IMR32 and Neuro2a cells upon KFL or ATRA treatment for 96 h was captured using phase contrast microscope equipped with monochrome camera. An increase in the number of cells bearing neurite like extensions upon treatment was observed. Representative image of experiments performed for three times. Scale bars = 67 μ m. (F) Cells bearing two or more neurites in IMR32 and Neuro2a cells treated with KFL (50 μ M) or ATRA (25 μ M) for 96 h were counted manually. The y-axis in the graph represents the percentage of cells bearing two or more neurites compared to the control cells treated with DMSO. The average \pm SEM from independent counting performed in 10 random focuses is shown (* $P < 0.05$; ** $P < 0.01$; *** $P < 0.001$; one-way ANOVA).

both IMR32- and Neuro2a-treated cells (Fig. 1B,C, D). An additional quantitation of the number of cells bearing two or more neurites indicated that an incubation period of 4 days is sufficient for KFL to effectively induce a significant change in the morphology (Fig. 1E,F), while in ATRA-treated cells there were lesser morphological changes in terms of neurite extensions when compared to KFL-treated cells. ATRA had been shown to require 10–14 days for a significant change in morphology [22], while KFL induced these changes in 4 days of treatment. Complementarily, we observed an increase in the mRNA and protein levels of certain neuron-specific marker genes like synaptophysin (*SYP*), neuron-specific enolase (*NSE*), and N-myc downregulated gene 1 (*NDRG1*; Fig. 2A,B). Although the mRNA transcripts of *NSE* and *NDRG1* in ATRA-treated condition did not show significant upregulation, the protein levels were upregulated during day 3 and day 4 of differentiation. The expression of N-myc, at mRNA level, was downregulated in KFL-treated conditions, while it was significantly increased in ATRA-treated conditions (Fig. 2A). In contrast, the downregulation of *N-myc* observed at the mRNA level was not exactly the same as observed at the protein level as there was no such drastic reduction in N-myc protein levels (Fig. 2B). The reason for this could be the accumulation of N-myc protein due to protein stabilization rather than transcription of the gene [23]. Moreover, the increase in the expression of N-myc protein is shown to be a required criterion for the onset of differentiation [24]. However, we observed an increase in *NDRG1* expression levels with a decrease in the expression level of N-myc protein between day 2 and day 4 (Fig. 2B); a phenomenon reported to occur during neuroblastoma differentiation [25]. Moreover, we analyzed the expression of apoptotic and proliferative marker genes upon KFL treatment in IMR32 cells (Fig. 2C). KFL treatment showed significant upregulation of apoptotic marker gene death receptor 5 (*DR5*) and tumor necrosis factor receptor type 1 (*TNFR1*). The upregulation of *DR5* upon KFL treatment had been reported in other cancer cells as a contributing factor for KFL induced cell death in cancer cells [26,27]. The significant upregulation of antiproliferative gene *p21* observed in our study supports the cease in the proliferation of IMR32 cells after KFL treatment. A downregulation of *Cyclin D1* expression was observed in both KFL and ATRA treatment (Fig. 2C). Altogether, our data suggest that KFL promotes differentiation and cell death in neuroblastoma cells.

Kaempferol-induced neuroblastoma differentiation is independent of the estrogen receptor signaling

It has been previously reported that KFL as a phytoestrogen (estrogen receptor agonist) suppresses the proliferation of breast cancer cells and promotes apoptosis and the use of an antagonist against estrogen receptors had shown to reverse the biological activity of KFL [28]. Since *ESR β* signaling has been shown to be essential for KFL-mediated biological responses [29], we examined the expression of *ESR α* and *ESR β* in IMR32 cells. In our study, we observed that KFL substantially induces the expression of estrogen receptor β (*ESR β*) compared to the estrogen receptor α (*ESR α*) both at mRNA level and at protein level in IMR32 cells (Fig. 3A,B). Investigations were carried out to determine if *ESR β* signaling is involved in the modulation of KFL-induced neuroblastoma differentiation. Hence, we used 4-[2-Phenyl-5,7-bis(trifluoromethyl)pyrazolo[1,5-*a*]pyrimidin-3-yl]phenol (PHTPP), a selective *ESR β* antagonist to find out if PHTPP pretreatment interfere with the differentiation process. Interestingly, pretreatment of KFL-treated cells with PHTPP had no effect both on the formation of neurites and β -III tubulin expression suggesting that KFL-induced differentiation is independent of *ESR β* signaling (Fig. 3C). Our results showed a basal expression of *ESR α* that was observed in IMR32 cells upon KFL pretreatment. Wang *et al.* [30] used tamoxifen to reverse this effect of KFL. Therefore, we performed an experiment with pretreatment of IMR32 cells with tamoxifen at different concentrations. Pretreatment of IMR32 cells with tamoxifen, an *ESR α* antagonist, also did not show any observable effects on the process of differentiation induced by KFL (data not shown). In addition, diarylpropionitrile (DPN), another *ESR β* agonist, failed to induce differentiation of IMR32 cells. Moreover, pretreatment with PHTPP did not reverse the cell death induced by KFL as well (Fig. 3D). Collectively, these findings suggest that KFL-induced neuroblastoma differentiation and cell death is not mediated by *ESR β* signaling.

Kaempferol modulates the expression of IRE1 α

Endoplasmic reticulum stress is known to be associated with cancer cell differentiation [31] and KFL has been known to induce ER stress in certain cancer cell lines [32,33]. These research findings prompted us to check the expression level of ER stress marker genes such as *BiP*, *PERK*, *IRE1 α* , and *ATF6* in KFL-treated IMR32 cells. The results presented in Fig. 4A show

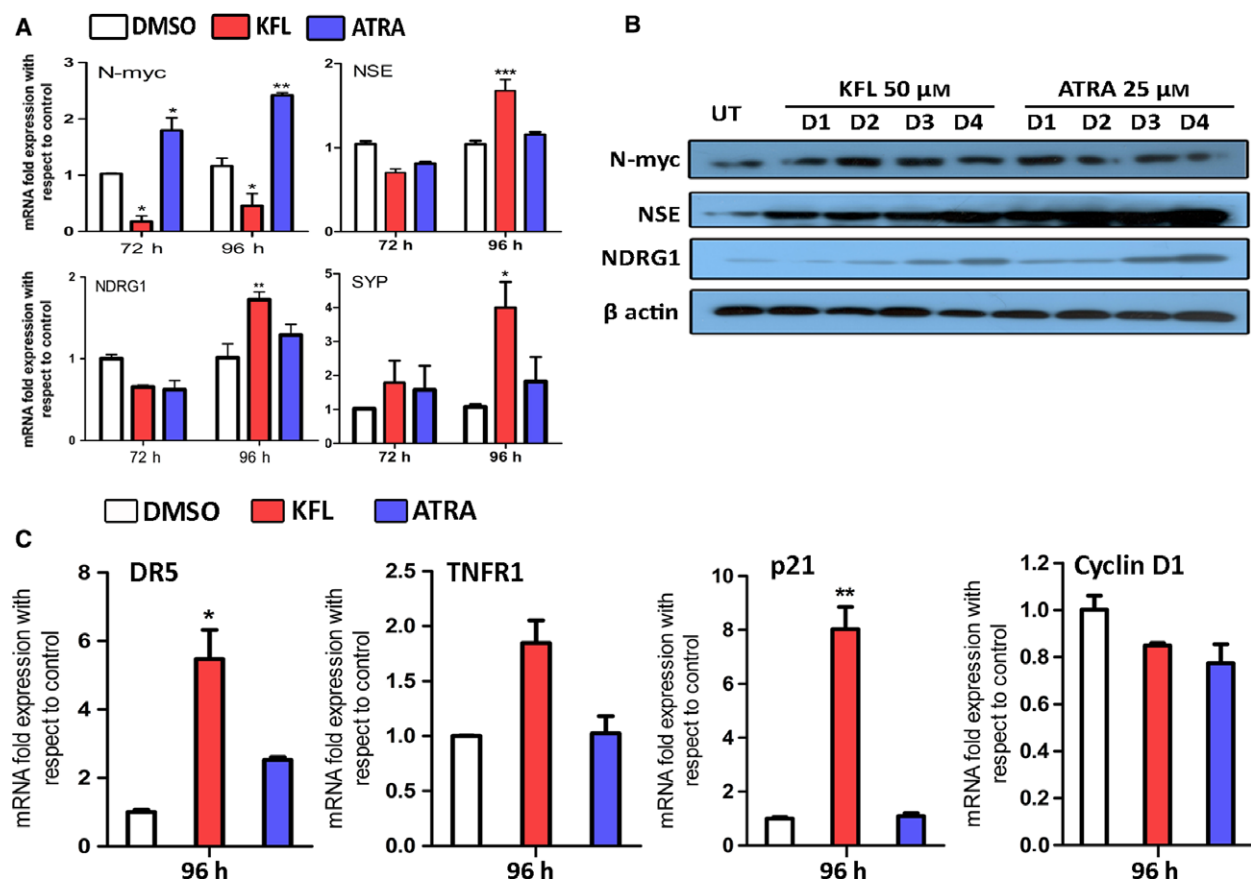


Fig. 2. KFL enhanced the expression of differentiation and apoptotic markers in IMR32 cells. (A) IMR32 cells were treated with KFL (50 μM) or ATRA (25 μM) and RNA was isolated at 72 and 96 h time points. Percent DMSO-treated cells at the respective time points were used as control. The mRNA expression of neuron-specific marker genes *SYP*, *NSE*, *NDRG1*, and *N-myc* in KFL- and ATRA-treated conditions were quantitated using qRT-PCR with 18s rRNA as internal control. Graphs represented as the average \pm SEM from three independent experiments (* P < 0.05; ** P < 0.01; *** P < 0.001; two-way ANOVA). (B) Proteins extracted from IMR32 cells treated with KFL (50 μM) or ATRA (25 μM) were analyzed using western blotting (50 μg of protein per lane) for the expression of NDRG1, NSE, and N-myc proteins. β actin served as loading control. (C) IMR32 cells were treated with KFL (50 μM) or ATRA (25 μM) and RNA was isolated at 96 h time point. The mRNA expression of *DR5*, *TNFR1*, *p21*, and *Cyclin D1* were quantified using qRT-PCR with 18s rRNA as internal control. DMSO-treated cells were used as control for normalization. Graphs are represented as the average \pm SEM from three independent experiments. (* P < 0.05; ** P < 0.01; *** P < 0.001; one-way ANOVA).

that KFL significantly increased the expression of *IRE1 α* , while not having a significant effect on other ER stress marker genes (Fig. 4A). *IRE1 α* is an ER transmembrane sensor of UPR pathway with both kinase and endoribonuclease activity. During ER stress, *IRE1 α* activation initiates the splicing of *XBP-1* mRNA which in turn gets translated into *XBP1s* protein that is involved in transcription of a diverse set of genes including genes involved in the UPR pathway [14]. Previous studies have reported the involvement of *IRE1 α* -*XBP1* pathway in the differentiation of plasma cells [16], osteoclasts [17], and adipocytes [18], in addition to the UPR pathway. This led us to hypothesize whether KFL might induce the neuroblastoma

differentiation by modulating the *IRE1 α* -*XBP1* pathway. We then performed protein analysis of *IRE1 α* for KFL-treated cells and compared it with brefeldin A (BFA; a known inducer of ER stress)-treated cells. Our results indicated that KFL increased the expression of *IRE1 α* but not BiP at protein level. BiP is a molecular chaperone and increase in the BiP levels is considered a hallmark of the ER stress process. In contrast, BFA treatment upregulated the expression levels of *IRE1 α* as well as BiP proteins indicating the onset of strong ER stress response (Fig. 4B). We have previously showed the bioactivity of KFL in ameliorating ER stress-induced cell death with a reduction in the expression level of ER stress markers in IMR32

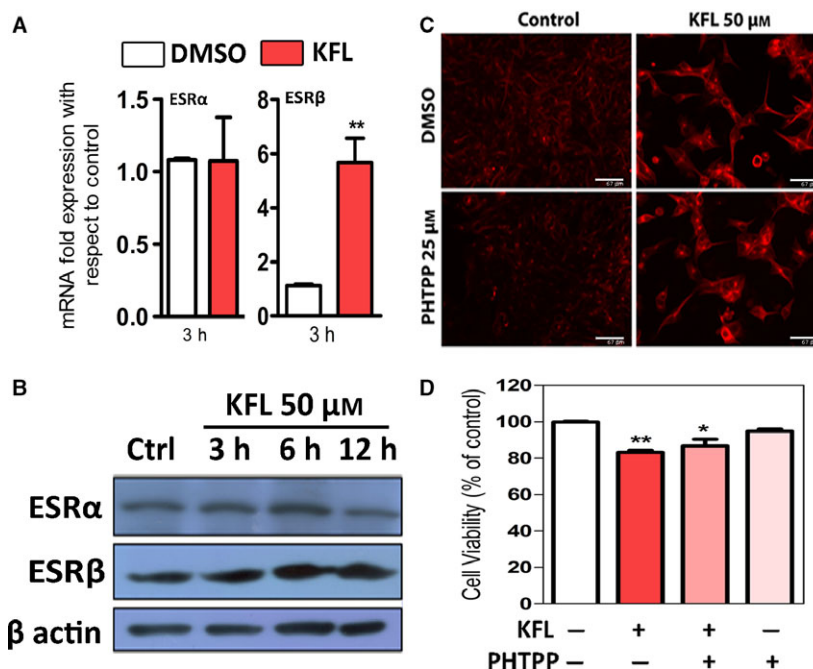


Fig. 3. Estrogen pathway independent activity of KFL. (A) IMR32 cells were treated with KFL (50 μ M) and total RNA was isolated at a early time point of 3 h after treatment. The mRNA expression levels of ESR α and ESR β upon KFL were quantified using qRT-PCR with 18s rRNA as internal control and DMSO-treated cells used for normalization. Graphs represented as the average \pm SEM from three independent experiments (* P < 0.05; ** P < 0.01; one-way ANOVA). (B) Proteins extracted from IMR32 cells treated with KFL (50 μ M) or DMSO (control) at 3 h, 6 h, and 12 h time points were analyzed using western blotting (50 μ g of protein per lane) with antibodies specific for the expression of ESR α and β . β actin served as the loading control. (C) IMR32 cells (seeded at a density of 50×10^3 cells per well in 12-well plate) were pretreated with PHTPP (an ER β antagonist) in the presence and absence of KFL. After 96 h of incubation, immunocytochemistry was performed to observe the increase in the expression of β III tubulin (red), a neuron-specific marker protein. Representative images of experiments performed for three times. Scale bars = 67 μ m. (D) IMR32 cells were treated with KFL (50 μ M) in the presence and absence of pretreatment with PHTPP. Cell death assay was performed using MTT. The y -axis shows the relative cell survival compared to DMSO-treated control cells. Results show no effect on the percent viability of cells pretreated with PHTPP (25 μ M) in presence of KFL. The graphs represent average \pm SEM from three independent experiments performed in triplicates (* P < 0.05; ** P < 0.01; one-way ANOVA).

cells upon pretreatment with KFL [20]. Our present study showed that KFL increased the expression of IRE1 α without activating ER stress in IMR32 cells.

Activation of IRE1 α endoribonuclease activity by kaempferol

Quercetin, a flavonoid, has been reported to bind to the Q-site in human-yeast chimeric IRE1 and activates endoribonuclease activity to enhance the cleavage of XBP1 mRNA [34]. KFL also belongs to the flavonoid class of phytochemicals. Considering this, we employed computational docking studies using Auto-dock to check if KFL binds to human IRE1 α molecule. Blind docking was performed by selecting the complete surface of the protein molecule. The result showed the KFL's binding affinity toward the kinase pocket of IRE1 α (Fig. 4C). The binding of KFL was

compared to bound states of indigenous activator of IRE1 α , ADP, and APY29 (known IRE1 kinase inhibitor and endoribonuclease activator; Fig. 4D). The bound state of ADP in the IRE1 α nucleotide binding site is known to activate the endoribonuclease activity of the molecule [35]. The docked poses analyzed for amino acid residues occupying the bound state of KFL showed that the binding of KFL to the kinase pocket of the molecule share the similar amino acid residues for interactions as of ADP and APY29 (Fig. 4D). The interactions of KFL with Glu 643, Cys 645, and His 692 residues of human IRE1 α had been shown for kinase activity inhibition by staurosporine (STS), a pan kinase inhibitor [36]. APY29 has been known to interact with amino acid residues of kinase domain to activate the endoribonuclease activity of IRE1 α [37]. Moreover, the interaction with Cys 645 at the kinase cleft has been reported for APY29 to

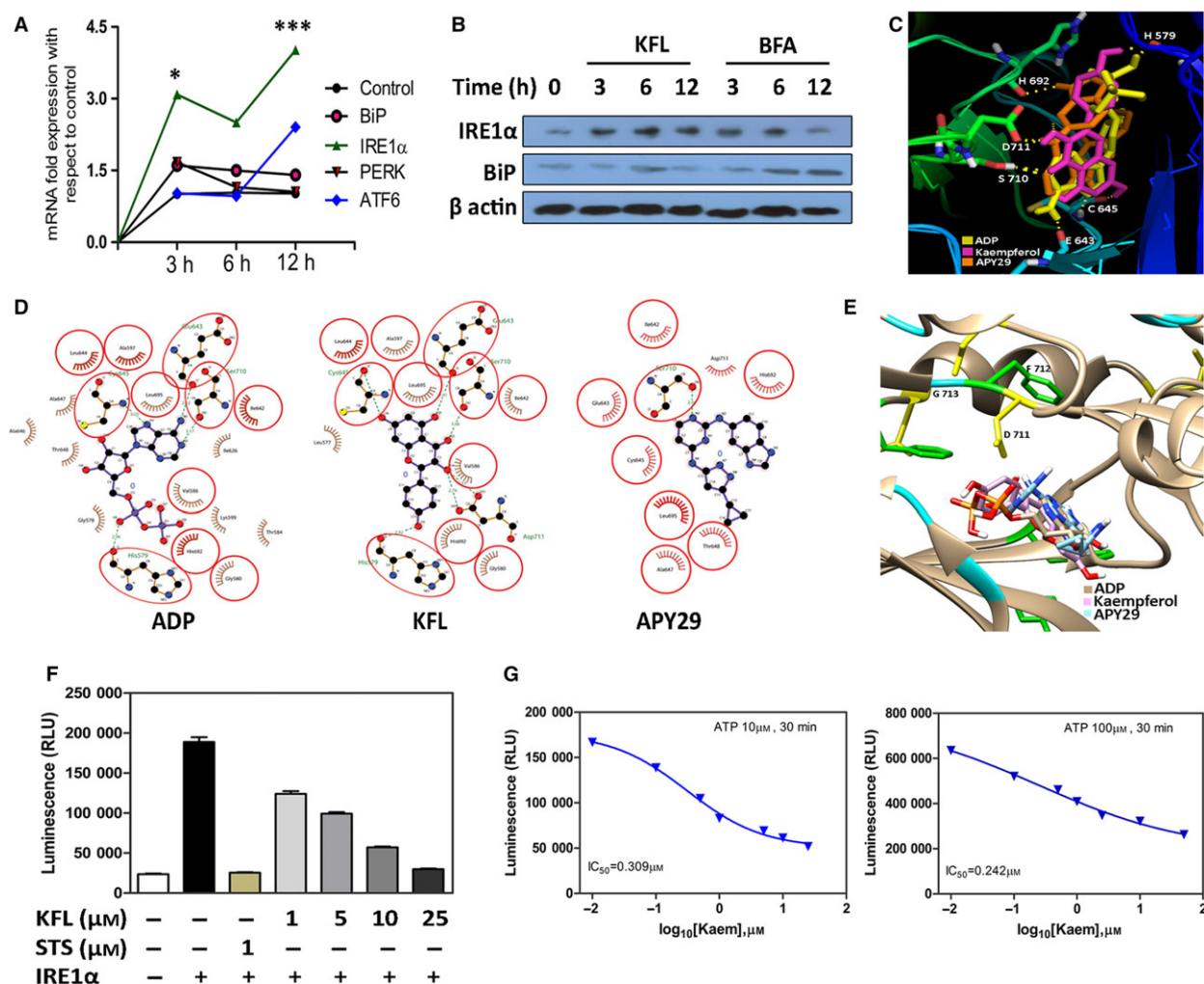


Fig. 4. IRE1 α modulation by KFL via binding to kinase domain. (A) IMR32 cells were treated with KFL (50 μ M) and total RNA was isolated at a 3, 6, and 12 h time points after treatment. The mRNA expression levels of *IRE1 α* , *BiP*, *PERK*, and *ATF6* upon KFL treatment were quantified using qRT-PCR. 18s rRNA was used as internal control and gene expression in DMSO-treated cells was used for normalization. Graphs represent the average \pm SEM from three independent experiments (* P < 0.05; *** P < 0.001; two-way ANOVA). (B) Proteins extracted from IMR32 cells treated with KFL (50 μ M) or BFA (1 μ g·mL⁻¹) at 3, 6, and 12 h time points were analyzed using western blotting (50 μ g of protein per lane) with antibodies specific for the expression of IRE1 α and BiP. β actin served as the loading control. (C) Docked poses of ADP, KFL, and APY29 at the nucleotide-binding site of human IRE1 α kinase domain obtained using AUTODOCK 4.0. Superimposed representation was made using PYMOL. Dashed yellow lines represent hydrogen bonding interactions. (D) LIGPLOT⁺ analysis (2D representation) of the docked complexes of ADP, KFL, and APY29. Red circles represent the common amino acid residues at the nucleotide binding site making interactions with all three compounds. Dashed green lines represent the hydrogen bonding between the amino acid residue and the compound. (E) Docked poses of ADP, KFL, and APY29 at the nucleotide binding site with DFG-in confirmation (D711, F712, and G713) in human IRE1 α (PDB ID: 3P23). Superimposed docked poses and interaction analysis was performed using UCSF chimera. (F) ADP-Glo assay for the IRE1 α kinase inhibition by KFL was performed by using different concentrations of KFL (1, 5, 10, and 25 μ M) against 50 ng of kinase active recombinant human IRE1 α enzyme per well. Reaction was performed in white, opaque 96-well plate. STS (1 μ M) was used as a positive control for kinase inhibition activity. Graphs representing the \pm SEM of experiment performed in triplicate. (G) Dose-dependent kinase inhibition assay performed using 10 or 100 μ M of ATP as substrate for IRE1 α kinase with different concentrations of KFL and 50 ng of IRE1 α enzyme per well. The x-axis plotted as log₁₀[kaem] represents the concentration of KFL and y-axis represents the relative light units (RLU). No significant change in the IC₅₀ value shows noncompetitive mode of binding of KFL to the kinase domain of human IRE1 α .

activate the IRE1 α endoribonuclease activity [38]. The conformation of DFG (Aspartic acid–Phenylalanine–Glycine) motif of kinase domain in IRE1 α with an activator for endoribonuclease activity should be in DFG-in conformation rather than DFG-out [38]. The ADP bound crystal structure of IRE1 α (PDB ID: 3P23), with DFG-in motif showing favorable binding affinity for docking with KFL suggests its ability to modulate the IRE1 α endoribonuclease activity. Moreover, docked pose of KFL falls into the same pocket where ADP and APY29 are known to interact with the kinase domain of IRE1 α (Fig. 4E). Collectively, docking analysis showed that KFL binds to the kinase domain of IRE1 α and could activate the endoribonuclease activity.

To confirm the docking results further, ADP-Glo kinase assay (Promega, Madison, WI, USA) was performed using recombinant kinase active human IRE1 α . Incubation of KFL with IRE1 α showed a dose-dependent decrease in the kinase activity of IRE1 α (Fig. 4F), confirming its binding to the kinase domain of the protein and thereby inhibiting IRE1 α 's kinase activity. The kinase inhibition assay performed by increasing the concentration of the substrate ATP from 10 to 100 μ M, suggested a noncompetitive mode of inhibition favored by KFL (Fig. 4G), which again correlates with the previously reported weak binding of quercetin [34] to the nucleotide binding site of human-yeast chimeric IRE1 protein.

IRE1 α knockdown reduces neuroblastoma differentiation

To further confirm the role of IRE1 α -XBP1 pathway in neuroblastoma differentiation, we established stable IRE1 α knockdown clones of IMR32 cells using lentiviral particles containing IRE1 α shRNA (four target-specific constructs that encodes 19–25 nucleotide shRNA). Successful knock down of IRE1 α at mRNA and protein level was confirmed by qRT-PCR and immunoblotting, respectively (Fig. 5A,B). The functional involvement of IRE1 α in neuroblastoma differentiation is confirmed, when neither KFL or APY29 treatment triggered β -III tubulin expression in IRE1 α knockdown IMR32 cells (Fig. 5C). Additionally, to compare the expression of neuronal differentiation markers (NDRG1 and NSE) between IRE1 α knockdown cells and control shRNA transduced cells, we performed immunoblotting analysis. We observed a decrease in the expression level of these markers in IRE1 α knockdown cells when compared to the control shRNA transduced cells (Fig. 5D). Also, we noticed a reduction in the XBP1s protein level in IRE1 α

shRNA-treated conditions on day 4, with a reduced level of differentiation observed. To confirm the endoribonuclease activity in inducing the differentiation of neuroblastoma cells, we inactivated the endoribonuclease activity of IRE1 α by using STF083010, a small molecule inhibitor. STF083010 is a specific inhibitor which binds to the endoribonuclease domain of IRE1 and inhibits the cleavage of XBP1 mRNA (Fig. 5E), while the kinase activity is left intact [39]. The extent of differentiation repression in IRE1 α knockdown cells, in the presence of KFL or APY29 was further enhanced by the addition of STF083010 (the IRE1 endoribonuclease inhibitor), to these cells (Fig. 5F). The number of cells with two or more neurites was significantly less in IRE1 α knockdown cells that are treated with either KFL or APY29, and this reduction in neurite growth was further decreased upon pretreatment with STF083010 (Fig. 5G). These results validate the role of IRE1 α 's endoribonuclease activity in KFL induced neuroblastoma differentiation.

XBP1s drives differentiation of neuroblastoma cells

Activated IRE1 α splices the *XBP1* mRNA, which then gets translated into an active transcription factor that regulates diverse set of genes involved in the regulation of various cellular processes including genes related to ER stress, differentiation, cell cycle arrest, and immune response. The ratio of spliced to unspliced form of XBP1 mRNA corresponds to the extent of IRE1 α activation. Small molecule modulators binding to the nucleotide binding site of IRE1 α can induce the endoribonuclease activity in the absence of ER stress [40].

Therefore, we decided to check the expression level of spliced *XBP1* mRNA by qRT-PCR. IMR32 cells were treated with KFL or BFA. While comparing the mRNA expression of *XBP1* unspliced to spliced form, we observed an enhanced XBP1 spliced mRNA levels upon KFL treatment. The increase in the expression of *XBP1* (unspliced) mRNA correlates with the enhanced expression of ATF6 [41] and this was not the case for BFA-treated cells as they displayed a decrease in the expression level of XBP1 unspliced form (Fig. 6A). To confirm that XBP1s protein is transcriptionally active, we analyzed its downstream targets such as *SEC63*, protein disulphide isomerase A 2 (*PDIA2*), *PDIA3*, DnaJ homolog subfamily C 3 (*DNAJC3*), endoplasmic reticulum DnaJ 4 and 5 (*ERDJ4* and *ERDJ5*) mRNA level by qRT-PCR, the regulation of these targets by the transcription factor XBP1s was validated before [42]. These downstream

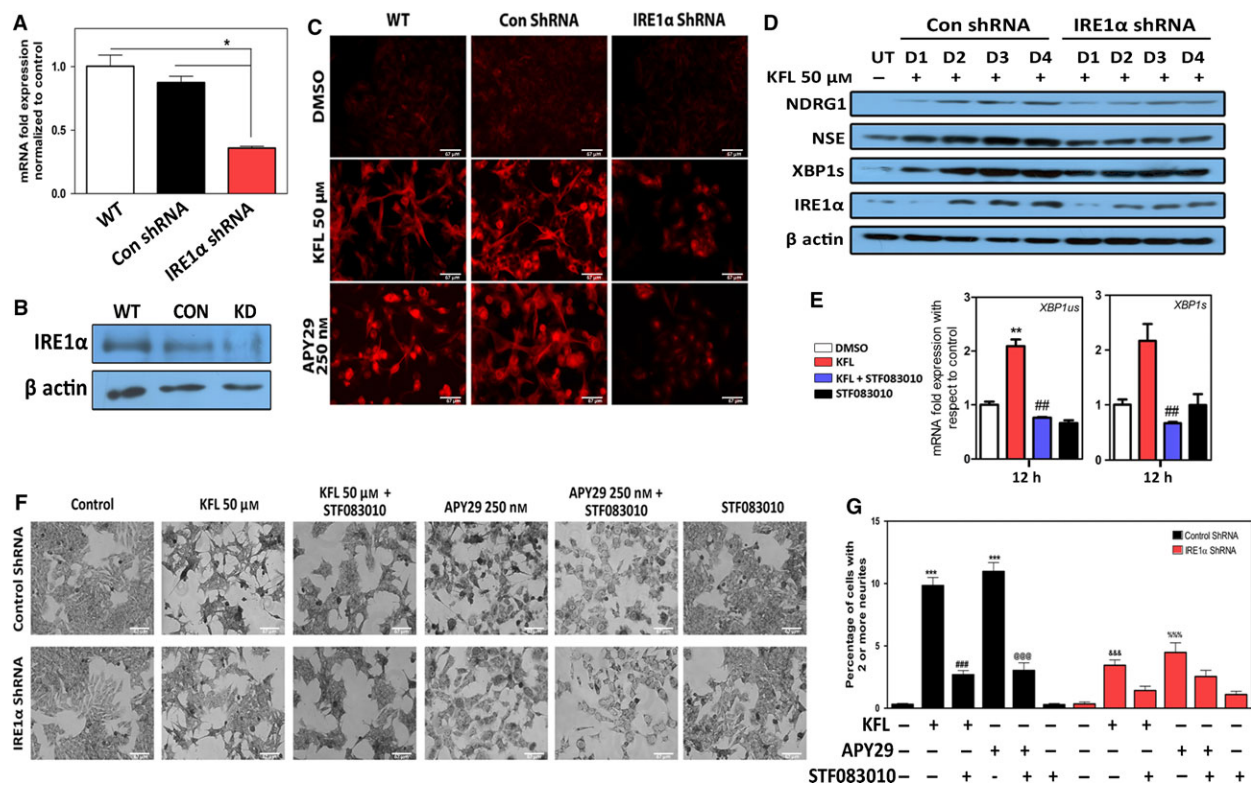


Fig. 5. IRE1 α knockdown reduced differentiation of IMR32 neuroblastoma cells. (A) Confirmation of knock down of IRE1 α at mRNA level in IMR32 cells transduced with shRNA lentiviral particles specific for IRE1 α . Total mRNA was extracted 12 h after the passaging the cells. The mRNA expression of IRE1 α was normalized with 18s rRNA expression as internal control. The graph represents average \pm SEM of experiment performed in triplicates (* P < 0.05; one-way ANOVA). (B) Proteins were extracted from IMR32 cells transduced with control shRNA and IRE1 α specific shRNA lentiviral particles. Western blotting analysis for the expression of IRE1 α knockdown was performed using IRE1 α specific antibodies with β actin as loading control. Representative blot of experiment performed for three times. IRE1 α shRNA-treated cells (KD) showing reduced expression than control shRNA (CON)-treated cells. (C) IMR32 cells transduced with control shRNA or IRE1 α shRNA seeded at a density of 50×10^3 cells per well in a 12-well plate were treated with KFL or APY29. After 96 h of incubation, immunocytochemistry was performed to observe the increase in the expression of β III tubulin (red), a neuron-specific marker protein. Representative images of experiments performed for three times. Scale bars = 67 μ m. Reduced expression of β III tubulin in IRE1 α knockdown IMR32 cells in the presence of KFL and APY29 was observed. (D) Proteins were extracted from IRE1 α shRNA transduced and control shRNA transduced IMR32 cells treated with KFL (50 μ M) at 24, 48, 72, and 96 h time points after the treatment. Western blotting analysis (50 μ g of protein per lane) was performed with antibodies specific for the expression of NSE, NDRG1, IRE1 α , and XBP1 proteins. Reduced expression of neuronal markers was observed in IRE1 α knockdown cells. Reduction in the expression of XBP1s levels was also observed in IRE1 α knockdown conditions. (E) IMR32 cells were treated with KFL in the presence and absence of pretreatment with STF083010 for 12 h and total RNA was isolated. Expression of *XBP1s* and *XBP1us* at mRNA level induced by KFL (50 μ M) in the presence of STF083010 (50 μ M) were quantified using qRT-PCR. The graph represents the average \pm SEM of three independent experiments. * represents the comparison between control and KFL-treated cells; # represents comparison between KFL-treated cells with STF083010-treated cells (* P < 0.05; ** P < 0.01; *** P < 0.001; one-way ANOVA). (F) IMR32 cells (control shRNA and IRE1 α -specific shRNA transduced) were treated with KFL or APY29 in the presence or absence of pretreatment with STF083010 (50 μ M) for 96 h and stained with methylene blue. Phase contrast methylene blue stained images of IMR32 cells depicting a change in morphology and neurite outgrowth were captured using a phase contrast microscope employed with monochrome camera. Pretreatment with STF083010 (50 μ M) inhibits the process of neuritogenesis further in IRE1 α shRNA-treated cells. Representative images of experiments performed for three times. Scale bar = 100 μ m. (G) Cells bearing two or more neurites in IMR32 cells transduced with control shRNA (black bars) or IRE1 α -specific shRNA (red bars) treated with KFL (50 μ M) or APY29 (250 nM) in the presence or absence of pretreatment with STF083010 (50 μ M) for 96 h. The y-axis in the graph represents the percentage of cells bearing two or more neurites compared to the control cells treated with DMSO. STF083010 pretreatment reduces the number of neurite bearing cells in both KFL and APY29-treated conditions further. The average \pm SEM from 10 independent counting is shown.* represents comparison between control and KFL/APY29-treated cells; # and @ represents comparison between KFL/APY29-treated cells with STF083010 pretreated cells; & and % represents comparison between KFL and APY29-treated conditions in control shRNA and IRE1 α shRNA-treated cells, respectively (* P < 0.05; ** P < 0.01; *** P < 0.001; two-way ANOVA).

targets of XBP1s transcription factor were not selected randomly; they have certain roles in the events pertaining to cellular differentiation. High *SEC63* expression has been shown to have an involvement in apoptosis and reduced proliferation in hepatic tumors [43]; ERDJ4 has been shown to have a crucial

role in B cell differentiation in the event of hematopoiesis [44]. Besides, *DNAJC3* levels are known to increase during plasma cells differentiation [45]; the expression of *PDIA3* and *DNAJC3* was shown to be upregulated during T-helper cell differentiation and treatment with IRE1 α 's endoribonuclease activity

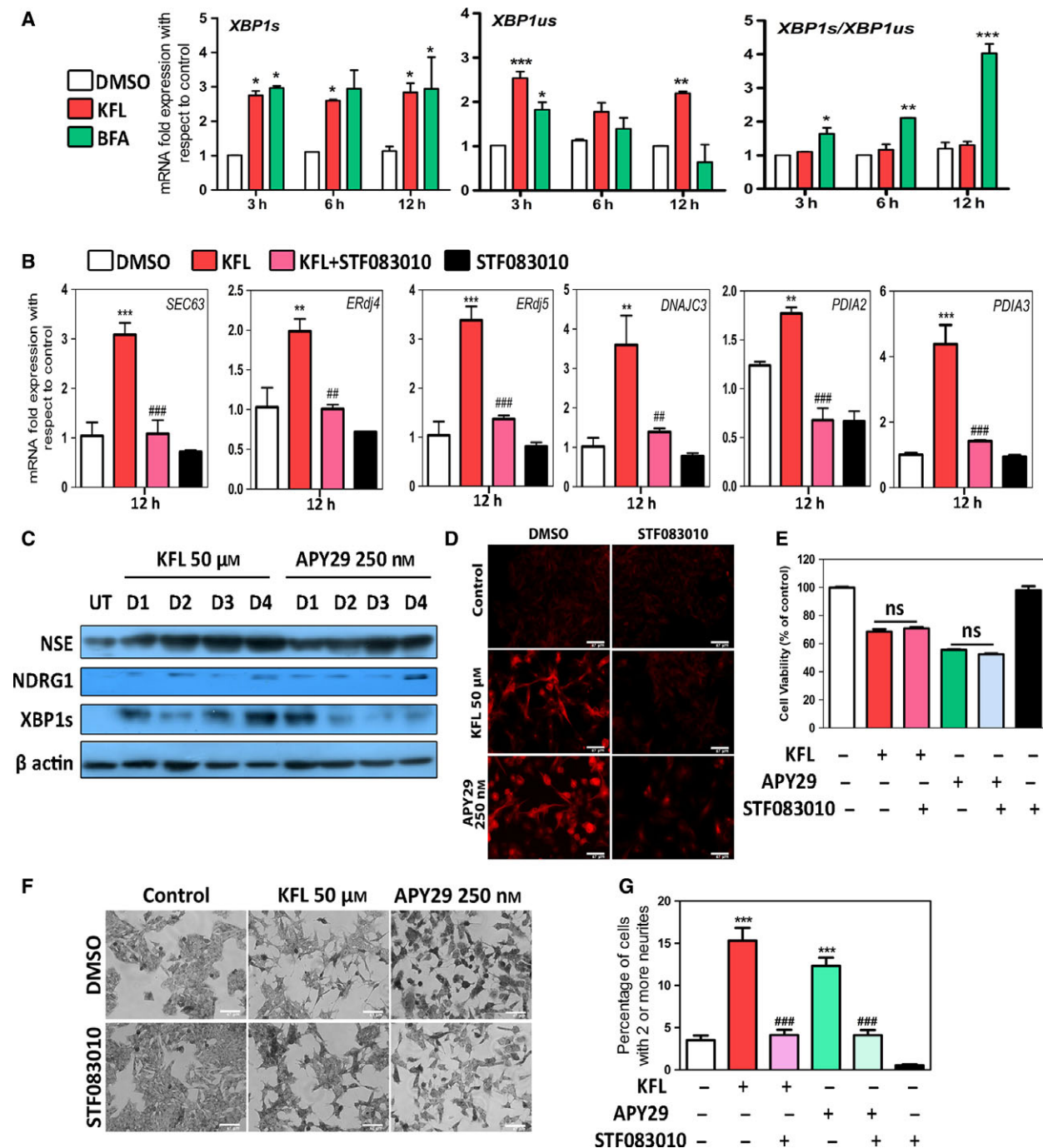


Fig. 6. Role of XBP1s expression in the differentiation of neuroblastoma. (A) IMR32 cells were treated with KFL (50 μM) or BFA (1 $\mu\text{g}\cdot\text{mL}^{-1}$) and total RNA was isolated at 3, 6, and 12 h time points. Graphs representing the spliced and unspliced form of *xbp1* mRNA present upon KFL and BFA treatment. Ratio represented to point out that KFL-treated cells maintains high expression levels of *xbp1* spliced and unspliced form. The graph represents the average \pm SEM from three independent experiments (* $P < 0.05$; ** $P < 0.01$; *** $P < 0.001$; two-way ANOVA). (B) IMR32 cells were treated with KFL in the presence and absence of STF083010 (50 μM). Total RNA was isolated after 12 h of treatment and gene expression studies on six downstream transcriptional targets (*SEC63*, *ERDJ4*, *ERDJ5*, *DNAJC3*, *PDIA2*, and *PDIA3*) of XBP1s were performed using qRT-PCR. 18s rRNA was used as internal control and gene expression was normalized with respect to the gene expression in DMSO-treated control cells. The average \pm SEM experiments performed in duplicates ($n = 3$). * represents comparison between control and KFL-treated cells; # represents comparison between KFL-treated cells with STF083010-treated cells (* $P < 0.05$; ** $P < 0.01$; *** $P < 0.001$; one-way ANOVA). (C) Proteins extracted at 24, 48, 72, and 96 h time points from IMR32 cells treated with KFL (50 μM) or APY29 (250 nM) were analyzed using western blotting (50 μg of protein per lane) with antibodies specific for the expression of NSE, NDRG1 and XBP1 proteins. An increase in the expression of neuron-specific marker expression was observed with increased XBP1s levels in KFL and APY29-treated conditions. (D) IMR32 cells seeded at a density of 50×10^3 cells per well in a 12-well plate were treated with KFL or APY29 in the presence and absence of pretreatment with STF083010 (a IRE1 α endoribonuclease specific inhibitor). After 96 h of incubation, immunocytochemistry was performed to observe the increase in the expression of β III tubulin (red), a neuron-specific marker protein. Results showed a reduced expression of β III tubulin upon pretreatment of cells with STF083010 (50 μM) in the presence of KFL and APY29. Representative images of experiments performed for three times. Scale bar = 67 μm . (E) IMR32 cells were treated with KFL (50 μM) in the presence and absence of pretreatment with STF083010 (50 μM) for 96 h. Cell death assay was performed using MTT. The y-axis shows the relative cell survival compared to DMSO-treated control cells. Results show no effect on the percent viability of cells pretreated with STF083010 (50 μM) in presence of KFL. The graphs represent average \pm SEM from three independent experiments performed in triplicates (* $P < 0.05$; ** $P < 0.01$; *** $P < 0.001$; one-way ANOVA). (F) IMR32 cells were treated with KFL or APY29 in the presence or absence of STF083010 (50 μM). Phase contrast methylene blue stained images of IMR32 cells show a change in morphology and neurite outgrowth upon treatment with KFL and APY29 for 96 h were captured using a microscope equipped with monochrome camera. Pretreatment with STF083010 (50 μM) inhibits the process of neuritogenesis. Representative images of experiments performed for three times. Scale bar = 67 μm . (G) Cells bearing two or more neurites in IMR32 cells treated with KFL (50 μM) or APY29 (250 nM) in the presence and absence of pretreatment with STF083010 for 96 h were counted manually. The y-axis in the graph represents the percentage of cells bearing two or more neurites compared to the control cells treated with DMSO. STF083010 pretreatment reduces the number of neurite bearing cells in both KFL- and APY29-treated conditions. The average \pm SEM from 10 independent counting is shown.* represents comparison between control and KFL/APY29-treated cells; # represents comparison between KFL/APY29-treated cells with STF083010 pretreated cells (* $P < 0.05$; ** $P < 0.01$; *** $P < 0.001$; one-way ANOVA).

specific inhibitor 4 μ8c downregulated their expression via inhibiting *XBPI* mRNA splicing [46]. Our results suggested that expression of all these genes increased in KFL-treated conditions, and get reversed by pretreatment with STF083010 (Fig. 6B). These results confirm that KFL activates XBP1s transcriptional activity by activating the endoribonuclease activity of IRE1 α and STF083010 blocks the transcriptional activity induced by KFL by inhibiting XBP1 mRNA cleavage. Furthermore, we proceeded to check whether APY29, an activator of IRE1 α endoribonuclease activity could induce the differentiation of IMR32 cells similar to KFL. Western blot analysis of APY29-treated cell lysates showed an increase in the expression of neuronal differentiation markers similar to that of KFL-treated conditions (Fig. 6C). STF083010 (50 μM) did not have cytotoxic effect in IMR32 cells; pretreatment with STF083010 followed by KFL treatment also did not modulate cell death (Fig. 6E) suggesting that cell death induction by KFL is independent of IRE1 α -XBP1 pathway. However, immunocytochemistry analysis for the expression of β -III tubulin showed reduced differentiation upon STF083010 pretreatment, in both KFL- and APY29-

treated conditions (Fig. 6D). In addition, there was a reduced change in morphology and a decrease in the number of cells bearing neurites with STF083010 pretreatment in the presence of KFL or APY29 (Fig. 6F, G). The induction of differentiation by APY29 observed in Neuro2a cells was similar to KFL-treated conditions. There was a marked increase in the β -III tubulin expression and SYP vesicles observed in immunocytochemistry experiments undertaken in Neuro2a cells (Fig. 7A,B). Taken together, these results suggest that KFL activates the IRE1 α -XBP1 branch pathway to induce the neuroblastoma differentiation. In addition, we analyzed if IRE1 α -XBP1 pathway is involved in inducing neuroblastoma differentiation by other agents like CDDO and ATRA [47]. However, we found that preincubation of cells with STF083010 did not inhibit differentiation induced by CDDO or ATRA (Fig. 8A,B) suggesting that IRE1 α activation is not the only pathway involved in neuroblastoma differentiation. Altogether, these results suggest that STF083010 inhibits differentiation but not cell death induced by KFL and APY29. Therefore, the activation of endoribonuclease activity of IRE1 α followed by the XBP1 mRNA splicing holds a crucial role in

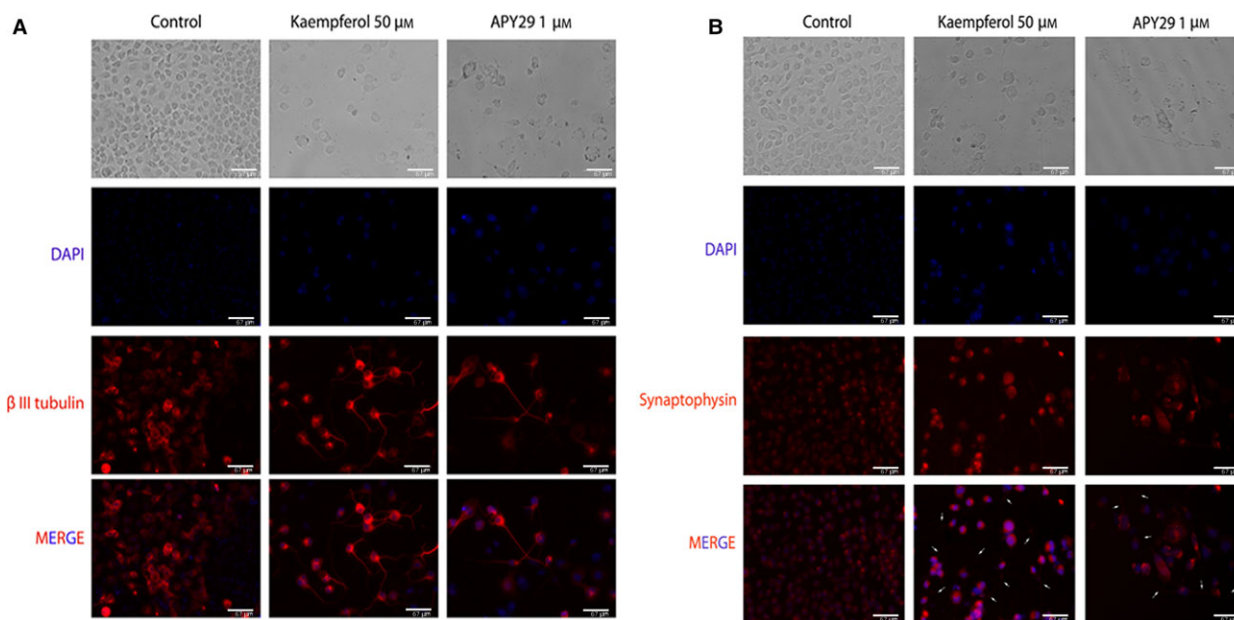


Fig. 7. KFL and APY29 induced differentiation of Neuro2a cells. (A, B) Neuro2a cells were treated with KFL or APY29 (a known activator of IRE1 α endoribonuclease activity) for 96 h and immunocytochemistry was performed for observing the expression of β III tubulin and SYP proteins. An increase in the expression of β III tubulin in cell body and SYP expression at neurites (white arrows) was observed in treated cells. Nuclear staining was done using DAPI (blue) and proteins by Alexa fluor 594 (red). DMSO-treated cells was used as control. Representative images of experiments performed more than three times. Scale bars = 67 μ m.

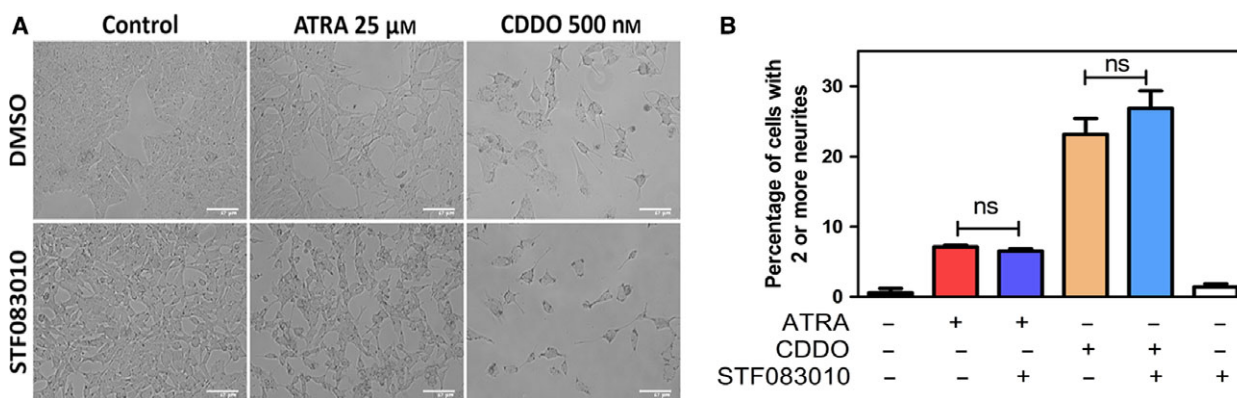


Fig. 8. STFO83010 inhibition of neuroblastoma differentiation is specific for KFL. (A) IMR32 cells (50×10^3) were seeded in 24-well plate and treated with ATRA 25 μ m or CDDO 500 nM in the presence or absence of STFO83010 (50 μ m) for a period of 5 days and change in the morphology was observed under phase contrast microscopy equipped with monochrome camera. Representative images of experiment performed for three times. Scale bar = 67 μ m. (B) Cells bearing two or more neurites in IMR32 cells treated with ATRA (25 μ m) or CDDO (500 nM) in the presence or absence of STFO83010 (50 μ m) for 5 days. The y-axis in the graph represents the percentage of cells bearing two or more neurites. STFO83010 (50 μ m) pretreatment did not reduce the number of neurite bearing cells in both ATRA- or CDDO-treated conditions. The average \pm SEM from five independent counting is shown (nonsignificant at $P < 0.05$; one-way ANOVA).

inducing the differentiation of neuroblastoma cells. This could be the reason for the morphological changes and neurite outgrowths observed earlier in other neuroblastoma cell lines upon treatment with flavonoids [48,49].

Discussion

Although several studies have been done in improving the prognosis of high-risk neuroblastoma with differentiation therapies, the survival rate of patients

remains considerably poor [50]. The implementation of chemotherapeutic approaches with synthetic molecules also adds up to the detrimental effects on the patients. Therefore, an enhanced understanding of differentiation pathways and novel therapeutic approaches are needed. An approach using dietary compounds or plant metabolites could be a better alternative for reducing the damaging effects of synthetic drugs. RA and its derivatives are well explored for their effects in inducing differentiation of neuroblastoma cells in clinical therapies. Other than RA, there are reports on the activity of 17 β -estradiol in enhancing the neuritogenesis in pheochromocytoma cells, *in vitro* [51]. Flavonoids, being known for their anticancer activity, mimic estrogen in physiological systems, while some of them have been reported to induce neuritogenesis in neuroblastoma cells *in vitro* [48,49]. KFL had been reported before for its anticancer activity via multiple cellular pathways which include upregulation of DR5 receptor expression via estrogen receptor expression and suppression of signal-regulated kinases [28].

The role of IRE1 α in differentiation of multiple cell types shows its involvement in deciding the fate of cells. *XBPI* mRNA, the major substrate for the IRE1 α endoribonuclease activity, has been shown to transcribe genes that are involved in multiple cellular processes, including genes involved in the differentiation of numerous cell types. The role of quercetin, a flavonoid, in activating the endoribonuclease activity of IRE1 α gave a hint to explore the anticancer activity of KFL in the viewpoint of the role of IRE1 α -*XBPI* pathway in the differentiation of neuroblastoma cells [34]. Moreover, the inactivation of IRE1 α endoribonuclease activity and the hypomorphic expression of *XBPI* in intestinal stem cells has been shown to be the reason for intestinal tumorigenesis [52].

The difference in the gene expression pattern between KFL- and ATRA-treated conditions shows that they both could activate different pathways to induce neuroblastoma differentiation. CDDO, a synthetic triterpenoid has been shown to induce differentiation of IMR32 cells via PPAR γ signaling pathway while ATRA has its effect via CREB dependent pathways [47]. The difference between the mRNA and protein expression of NSE observed in ATRA-treated condition was observed in other studies as well. The differentiation of SK-N-DZ cells by overexpression of the aryl hydrocarbon receptor showed no change in the regulation of NSE at transcript levels [53]. These data suggest that the transcripts of neuronal markers might be regulated via post-transcriptional regulatory mechanisms. Aside from the activation of IRE1 α - *XBPI* pathway, critical role of activation of other

signaling pathways such as cMAP and p38 mitogen-associated protein kinase (MAPK) pathway [54], JNK-MAPK pathway, and PPAR γ signaling pathway [47] have been reported to have a critical role in inducing the differentiation of neuroblastoma cells.

In summary, the current study demonstrated the involvement of IRE1 α in the differentiation of neuroblastoma cells. Modulation of IRE1 α in neuroblastoma cells by KFL, or by any specific modulator entitled for activating the endoribonuclease activity of IRE1 α , showed enhanced cell death, proliferation-repression coupled to differentiation, with increase in expression of neuronal markers, all of which are expected outcomes of neuroblastoma therapies. The results presented herein demonstrate that KFL induces differentiation and cell death of neuroblastoma cells. Also, present study suggests a new therapeutic approach via modulation of IRE1 α for the treatment of neuroblastoma.

Materials and methods

Cell culture and reagents

IMR32, a human neuroblastoma cell line, and Neuro2A, a mouse neuroblastoma cell line, were obtained from NCCS, Pune, India. Cells were maintained in Dulbecco's modified Eagle's medium containing 10% FBS (Himedia, Mumbai, India), 1 \times glutamine and 1 \times antibiotic and antimycotic solution at 37 °C and 5% CO₂. KFL (HPLC purity \geq 98.8%) was obtained from Natural remedies (Bangalore, India). DPN and 4-[2-Phenyl-5,7-bis(trifluoromethyl)pyrazolo[1,5-*a*] pyrimidin-3-yl] phenol (PHTPP) were obtained from Alfa Aesar (Hyderabad, India). APY29 was purchased from MedChem express (Monmouth Junction, NJ, USA). STF083010 was purchased from Cayman chemicals (Ann Arbor, MI, USA).

Cell viability assay

MTT assay was performed for analyzing the cytotoxic effect of KFL on IMR32 and Neuro2A cell lines. Briefly, 0.5×10^4 cells were seeded per well in a 96-well plate and treated with KFL for 48, 72, and 96 h. After the desired incubation time, 20 μ L of 5 mg·mL⁻¹ MTT (Himedia) was added to each of the well and incubated for 3 h. The tetrazolium salt formed by the live cells was dissolved by adding 200 μ L of DMSO, after the removal of media. The purple color formed was read at 570 nm using ELISA plate reader.

Cell proliferation assay

For trypan blue dye exclusion assay, 0.5×10^5 cells per well were seeded in a 24-well plate. Cells were treated with different concentrations KFL (25, 50 and 100 μ M), ATRA

(25 μM), and DMSO (vehicle) for a period of 48, 72, and 96 h. Cell counting was done manually using haemocytometer, by staining the cells with trypan blue solution prepared in 0.4% methanol. Live cells that did not take up the dye were counted to quantitate the rate of proliferation under control and treated conditions.

Differentiation experiments

For differentiation experiments, neuroblastoma cell lines were seeded at a density of 3×10^5 cells in 60 mm dish and treated with 50 μM of KFL. Induction was given once for a continuous time of 96 h without any replacement of media. ATRA at a concentration of 25 μM was used as a positive control to compare the morphological changes; images were taken using phase contrast microscope at specified time points.

Stable lentiviral transductions

The IRE1 α (sc-40705-V) shRNA lentiviral particles purchased from Santa Cruz Biotechnology (Santa Cruz, CA, USA) contain expression constructs encoding target-specific shRNA designed to specifically knock down human IRE1 α gene expression. Scrambled shRNA contained lentiviral particles (sc-108080; Santa Cruz Biotechnology) that do not lead to specific degradation of any cellular mRNA and was used as negative control. Lentiviral transduction was performed in the presence of polybrene (5 $\mu\text{g}\cdot\text{mL}^{-1}$; Sigma-Aldrich, St. Louis, MO, USA), and stable transductants were generated via selection with puromycin (1 $\mu\text{g}\cdot\text{mL}^{-1}$; Sigma-Aldrich) according to the manufacturer's instructions.

Immunocytochemistry and microscopy

Immunocytochemistry was carried out as described in the Cell signaling Technology (CST) guide. Briefly, 2.5×10^4 cells per well were seeded in a 24-well plate. After overnight incubation, cells were treated with the compounds for indicated time. Cells were then washed with $1 \times$ PBS and fixed with 4% formaldehyde for 15 min. Cells were washed again with $1 \times$ PBS and incubated with 0.5% skimmed milk containing 0.3% triton X-100 for blocking nonspecific binding, for 1 h. Immunostaining was done using β -III tubulin (CST #5568) and SYP (Novus, Centennial, CO, USA; #NB2-25170SS) specific primary antibodies at 4 $^{\circ}\text{C}$ with overnight incubation followed by 1-h incubation with the secondary antibody, anti-rabbit Alexa Flour 594 (#8889; Cell Signaling Technologies, Beverly, MA, USA). Phase contrast and fluorescence images of cells under treated and nontreated conditions were captured using EVOS FLoid imaging station (Thermo Fischer, Waltham, MA, USA) with $20 \times$ fluorite objective and LED light cubes containing hard coated filters (blue and red). For a particular protein expression study, imaging parameters were kept constant throughout the imaging and no image modifications were done post-imaging.

Gene expression analysis

Total RNA isolation was performed using RNA isoplus (Takara, New Delhi, India). RNA quantification was performed and 2 μg of total RNA was used for cDNA conversion using Primescript RT reagent kit (Takara). Quantitative-PCR (qRT-PCR) was performed using SYBR green reagent (Takara) using Applied Biosystems (Waltham, MA, USA) Quant studio 3 real-time PCR

Table 1. List of primers used in this study.

| Gene | Sense (5'–3') | Anti-sense (5'–3') |
|--------------------------------|---------------------------|----------------------------|
| <i>18s</i> | GCCGCTAGAGGTGAAATCT | CATTCTTGGCAAATGCTTTC |
| <i>BiP</i> | CAACCAACTGTTACAATCAAGGTC | CAAAGGTGACTTCAATCTGTGG |
| <i>IRE1α</i> | CCATCGAGCTGTGTGACG | TGTTGAGGGAGTGGAGGTG |
| <i>ATF6</i> | GGCATTATAATACTGAACATATGGA | TTTGATTGTCAGGGCTCAC |
| <i>PERK</i> | CAGTGGGATTTGGATGTGG | GGAATGATCATCTTATTTCCAAA |
| <i>XBP1α</i> | CCGCGAGCACTCAGACTACG | ATGTTCTGGAGGGGTGACAA |
| <i>XBP1β</i> | CCGCGAGCAGGTGCAGG | GAGTCAATACCGCCAGAATCCA |
| <i>Sec63</i> | CCTCCACTTACCTGCCATA | GGTTCCGGGCCATTACTATF |
| <i>PDIA2</i> | GATCAGCGGCCAGTTAAGAC | GATGTCCTCGTGGTCTTGGT |
| <i>PDIA3</i> | AAGCTCAGCAAAGACCCAAA | CACTTAATTCACGGCCACCT |
| <i>ERdj4</i> | TCGGCATCAGAGCGCAAATCA | ACCACAGTAAAAGCACTGTGTCCAAG |
| <i>ERdj5</i> | GACGGGCAAAGATGTCAGGA | GCCCGTTTGGCCTTTTCTAC |
| <i>DNAJC3</i> | CTCAGTTTCATGCTGCCGTA | TTGCTGCAGTGAAGTCCATC |
| <i>DR5</i> | AGGTGAAGTGGAGCTAAGTC | TCACTCCAGGGTGTACAATC |
| <i>TNFR1</i> | CGCTACCAACGGTGGAAAGTC | CAAGCTCCCCCTCTTTTTCAG |
| <i>p21</i> | CATGTGGACCTGCTACTGTCTTGTA | GAAGATCAGCCGGCGTTTG |
| <i>CyclinD1</i> | ATGTTTCGTGGCCTTAAGATGA | CAGGTTCCACTTGAGCTTGTTTC |

machine. Human 18s rRNA was used as an internal control for normalizing the gene expression. The fold-induction of mRNA levels was calculated by $2^{-\Delta\Delta CT}$ method. The list of primers used in this study is tabulated (Table 1).

Immunoblotting

Immunoblotting was carried out as described earlier by Ravanan *et al.* [55]. In brief, cells were plated in 60 mm dishes at the density of 1.5×10^5 cells per dish. After overnight incubation, cells were treated with the above-mentioned compounds. At 24, 48, 72, and 96 h time points after the treatment, cells were washed with ice-cold PBS and lysed with RIPA buffer containing $1 \times$ Protease inhibitor cocktail (Sigma Aldrich). Total protein concentrations were quantified by Folin's assay. Immunoblotting analysis was done by loading 50 μ g of protein in each lane for SDS/PAGE analysis. Antibodies used in this study were obtained from Cell Signalling Technology (β actin#8457, N-myc#9405, IRE1 α #3294 and XBP1s#12782), Novus biological (NDRG1#NBP1-32074, ER α #NB120-3577, and ER β #NB100-92166), and ABclonal (Woburn, MA, USA) (NSE #A3118 and GRP78 #A0241). Anti-rabbit, HRP-linked secondary antibody from Cell Signalling Technology (#7074) was used for chemiluminescence-based detection.

Methylene blue staining and neurite counting

Cells were seeded in 35 mm dish at a density of 1.5×10^5 cells and differentiation was induced with KFL (50 μ M) or APY29 (250 nM). Wherever STF083010 (50 μ M) is used as inhibitor, cells were pretreated with STF083010 for 90 min and then treated with the above mentioned test compounds. After 96 h of incubation, cells were fixed using 4% formaldehyde for 15 min and stained using 0.2% methylene blue solution in methanol for 30 min. After repeated washes for unbound stain removal, images were taken using monochrome phase contrast camera of EVOS FLoid imaging station (Thermo Fischer). Total number of cells and cells bearing two or more neurites were counted in 10 random fields and represented as percentage of cells in the graph [47].

Kinase inhibition studies

Recombinant human IRE1 α enzyme was obtained from SignalChem (Burlington, NC, USA) (#E31-11G). ADP-Glo kinase assay (Promega) was performed as per the manufacturer's protocol to confirm the inhibitory mechanism of KFL. Briefly, 50 ng of enzyme was used with 10 or 100 μ M of ATP with different concentrations of KFL in a white flat bottom 96-well plate. STS (Sigma Aldrich),

a pan kinase inhibitor, was used as a positive control. The luminescence produced by the conversion of dephosphorylated ADP to ATP was measured using the luminometer (Berthold, Bad Wildbad, Germany).

In silico docking analysis

Studies to understand the mode of binding of KFL to IRE1 α was carried out using AUTODOCK SUITE 4.0 (The Scripps Research Institute, La Jolla, CA, USA). Crystal structure of the human IRE1 α bound with ADP (PDB ID: 3P23) was used as the target protein. Ligands were obtained from Pubchem as.sdf format and converted to.pdb using smiles translator. Polar hydrogen atoms were assigned for the macromolecule prior docking. Gasteiger charges for ligands and Kollman charges for the receptor molecule was added using AUTODOCK TOOLS 1.5.6 (The Scripps Research Institute). Throughout the study, the macromolecule was kept rigid with rotatable bonds assigned for the ligands. The grid center made on the macromolecule covering the entire surface of the protein acted as search space. AUTOGRID 4.0 was used to produce the map files of the flexible atoms and docking parameter file was generated using Lamarckian Genetic algorithm of AUTODOCK 4.0 (The Scripps Research Institute). Validation of the docking study was carried out by re-docking the ADP with the solved crystal structure of kinase domain of IRE1 α . The re-docked complex was compared to the known crystal structure of the ligand–macromolecule complex. Binding energies of the best docked pose of the docked complexes were calculated based on torsional energy, H-bonding, nonbonded interactions, and desolvation energies. LIGPLOT⁺ v. 1.4 (Thornton group, EMBL-EBI, Cambridgeshire, UK) was used to study the interactions at 2D level, while UCSF CHIMERA 1.10.2 (UCSF, San Francisco, CA, USA) and PYMOL v. 1.7.4 (Schrödinger, Cambridge, MA, USA) were used in visualizing 3D interactions.

Statistical analysis

All data are presented as the standard error of mean (SEM) of at least three independent experiments. Statistical comparisons were performed using one-way/two-way analysis of variance (ANOVA) followed by Bonferroni's multiple comparison test (GRAPHPAD PRISM, version 5.0, Graphpad Software, San Diego, CA, USA) and *P*-value of < 0.05 was considered statistically significant.

Acknowledgements

PR greatly acknowledges DST-SERB for the financial support through the Research Grant- SB/FT/LS-419/2012. We thank Ms. Ida Florance PS for her kind help in counting cells bearing neurites.

Conflicts of interest

The authors declare no conflict of interest.

Author contributions

PR conceived and designed the experiments and AA performed all the experiments. Data analysis and manuscript preparation was done by PR, AA. PT and CL contributed in the discussion.

References

- 1 Hoehner JC, Gestblom C, Hedborg F, Sandstedt B, Olsen L & Pahlman S (1996) A developmental model of neuroblastoma: differentiating stroma-poor tumors' progress along an extra-adrenal chromaffin lineage. *Lab Invest* **75**, 659–675.
- 2 Ross RA, Biedler JL & Spengler BA (2003) A role for distinct cell types in determining malignancy in human neuroblastoma cell lines and tumors. *Cancer Lett* **197**, 35–39.
- 3 Brodeur GM (2003) Neuroblastoma: biological insights into a clinical enigma. *Nat Rev Cancer* **3**, 203–216.
- 4 Matthay KK, Villablanca JG, Seeger RC, Stram DO, Harris RE, Ramsay NK, Swift P, Shimada H, Black CT, Brodeur GM *et al.* (1999) Treatment of high-risk neuroblastoma with intensive chemotherapy, radiotherapy, autologous bone marrow transplantation, and 13-cis-retinoic acid. Children's Cancer Group. *N Engl J Med* **341**, 1165–1173.
- 5 Takahashi J, Palmer TD & Gage FH (1999) Retinoic acid and neurotrophins collaborate to regulate neurogenesis in adult-derived neural stem cell cultures. *Dev Neurobiol* **38**, 65–81.
- 6 Reynolds CP, Matthay KK, Villablanca JG & Maurer BJ (2003) Retinoid therapy of high-risk neuroblastoma. *Cancer Lett* **197**, 185–192.
- 7 Pemrick SM, Lucas D & Grippo J (1994) The retinoid receptors. *Leukemia* **8**, S1–S10.
- 8 Halder D, Kim GH & Shin I (2015) Synthetic small molecules that induce neuronal differentiation in neuroblastoma and fibroblast cells. *Mol BioSyst* **11**, 2727–2737.
- 9 Lange C, Mix E, Frahm J, Glass A, Müller J, Schmitt O, Schmöle A-C, Klemm K, Ortinau S & Hübner R (2011) Small molecule GSK-3 inhibitors increase neurogenesis of human neural progenitor cells. *Neurosci Lett* **488**, 36–40.
- 10 Kollareddy M, Sherrard A, Park JH, Szemes M, Gallacher K, Melegh Z, Oltean S, Michaelis M, Cinatl J Jr, Kaidi A *et al.* (2017) The small molecule inhibitor YK-4-279 disrupts mitotic progression of neuroblastoma cells, overcomes drug resistance and synergizes with inhibitors of mitosis. *Cancer Lett* **403**, 74–85.
- 11 Lu J, Guan S, Zhao Y, Yu Y, Woodfield SE, Zhang H, Yang KL, Bierkekehazhi S, Qi L, Li X *et al.* (2017) The second-generation ALK inhibitor alectinib effectively induces apoptosis in human neuroblastoma cells and inhibits tumor growth in a TH-MYCIN transgenic neuroblastoma mouse model. *Cancer Lett* **400**, 61–68.
- 12 Abdullah A & Ravanan P (2018) The unknown face of IRE1alpha - beyond ER stress. *Eur J Cell Biol* **97**, 359–368.
- 13 Urano F, Wang X, Bertolotti A, Zhang Y, Chung P, Harding HP & Ron D (2000) Coupling of stress in the ER to activation of JNK protein kinases by transmembrane protein kinase IRE1. *Science* **287**, 664–666.
- 14 Acosta-Alvear D, Zhou Y, Blais A, Tsikitis M, Lents NH, Arias C, Lennon CJ, Kluger Y & Dynlacht BD (2007) XBP1 controls diverse cell type- and condition-specific transcriptional regulatory networks. *Mol Cell* **27**, 53–66.
- 15 Iwawaki T, Akai R, Yamanaka S & Kohno K (2009) Function of IRE1 alpha in the placenta is essential for placental development and embryonic viability. *Proc Natl Acad Sci USA* **106**, 16657–16662.
- 16 Reimold AM, Iwakoshi NN, Manis J, Vallabhajosyula P, Szomolanyi-Tsuda E, Gravalles EM, Friend D, Grusby MJ, Alt F & Glimcher LH (2001) Plasma cell differentiation requires the transcription factor XBP-1. *Nature* **412**, 300–307.
- 17 Tohmonda T, Miyauchi Y, Ghosh R, Yoda M, Uchikawa S, Takito J, Morioka H, Nakamura M, Iwawaki T, Chiba K *et al.* (2011) The IRE1alpha-XBP1 pathway is essential for osteoblast differentiation through promoting transcription of Osterix. *EMBO Rep* **12**, 451–457.
- 18 Sha H, He Y, Chen H, Wang C, Zenno A, Shi H, Yang X, Zhang X & Qi L (2009) The IRE1alpha-XBP1 pathway of the unfolded protein response is required for adipogenesis. *Cell Metab* **9**, 556–564.
- 19 Wang J, Fang X, Ge L, Cao F, Zhao L, Wang Z & Xiao W (2018) Antitumor, antioxidant and anti-inflammatory activities of kaempferol and its corresponding glycosides and the enzymatic preparation of kaempferol. *PLoS ONE* **13**, e0197563.
- 20 Abdullah A & Ravanan P (2018) Kaempferol mitigates endoplasmic reticulum stress induced cell death by targeting caspase 3/7. *Sci Rep* **8**, 2189.
- 21 Chen AY & Chen YC (2013) A review of the dietary flavonoid, kaempferol on human health and cancer chemoprevention. *Food Chem* **138**, 2099–2107.
- 22 Pence JC & Shorter NA (1990) *In vitro* differentiation of human neuroblastoma cells caused by vasoactive intestinal peptide. *Can Res* **50**, 5177–5183.
- 23 Choi SH, Wright JB, Gerber SA & Cole MD (2010) Myc protein is stabilized by suppression of a novel E3 ligase complex in cancer cells. *Genes Dev* **24**, 1236–1241.

- 24 Guglielmi L, Cinnella C, Nardella M, Maresca G, Valentini A, Mercanti D, Felsani A & D'Agnano I (2014) MYCN gene expression is required for the onset of the differentiation programme in neuroblastoma cells. *Cell Death Dis* **5**, e1081.
- 25 Kang JH, Rychahou PG, Ishola TA, Qiao J, Evers BM & Chung DH (2006) MYCN silencing induces differentiation and apoptosis in human neuroblastoma cells. *Biochem Biophys Res Commun* **351**, 192–197.
- 26 Zhao Y, Tian B, Wang Y & Ding H (2017) Kaempferol sensitizes human ovarian cancer cells-OVCAR-3 and SKOV-3 to tumor necrosis factor-related apoptosis-inducing ligand (TRAIL)-induced apoptosis via JNK/ERK-CHOP pathway and up-regulation of death receptors 4 and 5. *Med Sci Monit* **23**, 5096–5105.
- 27 Gao Y, Yin J, Rankin GO & Chen YC (2018) Kaempferol induces G2/M cell cycle arrest via checkpoint kinase 2 and promotes apoptosis via death receptors in human ovarian carcinoma A2780/CP70 Cells. *Molecules* **23**, 1095.
- 28 Kim SH & Choi KC (2013) Anti-cancer effect and underlying mechanism (s) of kaempferol, a phytoestrogen, on the regulation of apoptosis in diverse cancer cell models. *Toxicol Res* **29**, 229–234.
- 29 Kuiper GG, Lemmen JG, Carlsson B, Corton JC, Safe SH, Van Der Saag PT, Van Der Burg B & Gustafsson J-A (1998) Interaction of estrogenic chemicals and phytoestrogens with estrogen receptor β . *Endocrinology* **139**, 4252–4263.
- 30 Wang J, Fang F, Huang Z, Wang Y & Wong C (2009) Kaempferol is an estrogen-related receptor alpha and gamma inverse agonist. *FEBS Lett* **583**, 643–647.
- 31 Wielenga MC, Colak S, Heijmans J, de Jeude JFL, Rodermond HM, Paton JC, Paton AW, Vermeulen L, Medema JP & van den Brink GR (2015) ER-stress-induced differentiation sensitizes colon cancer stem cells to chemotherapy. *Cell Rep* **13**, 489–494.
- 32 Huang WW, Chiu YJ, Fan MJ, Lu HF, Yeh HF, Li KH, Chen PY, Chung JG & Yang JS (2010) Kaempferol induced apoptosis via endoplasmic reticulum stress and mitochondria-dependent pathway in human osteosarcoma U-2 OS cells. *Mol Nutr Food Res* **54**, 1585–1595.
- 33 Guo H, Ren F, Zhang L, Zhang X, Yang R, Xie B, Li Z, Hu Z, Duan Z & Zhang J (2016) Kaempferol induces apoptosis in HepG2 cells via activation of the endoplasmic reticulum stress pathway. *Mol Med Rep* **13**, 2791–2800.
- 34 Wiseman RL, Zhang Y, Lee KP, Harding HP, Haynes CM, Price J, Sicheri F & Ron D (2010) Flavonol activation defines an unanticipated ligand-binding site in the kinase-RNase domain of IRE1. *Mol Cell* **38**, 291–304.
- 35 Lee KP, Dey M, Neculai D, Cao C, Dever TE & Sicheri F (2008) Structure of the dual enzyme Ire1 reveals the basis for catalysis and regulation in nonconventional RNA splicing. *Cell* **132**, 89–100.
- 36 Concha NO, Smallwood A, Bonnette W, Totoritis R, Zhang G, Federowicz K, Yang J, Qi H, Chen S & Campobasso N (2015) Long-range inhibitor-induced conformational regulation of human IRE1 α endoribonuclease activity. *Mol Pharmacol* **88**, 1011–1023.
- 37 Korennykh AV, Egea PF, Korostelev AA, Finer-Moore J, Zhang C, Shokat KM, Stroud RM & Walter P (2009) The unfolded protein response signals through high-order assembly of Ire1. *Nature* **457**, 687.
- 38 Wang L, Perera BGK, Hari SB, Bhatarai B, Backes BJ, Seeliger MA, Schürer SC, Oakes SA, Papa FR & Maly DJ (2012) Divergent allosteric control of the IRE1 α endoribonuclease using kinase inhibitors. *Nat Chem Biol* **8**, 982–989.
- 39 Papandreou I, Denko NC, Olson M, Van Melckebeke H, Lust S, Tam A, Solow-Cordero DE, Bouley DM, Offner F, Niwa M *et al.* (2011) Identification of an Ire1 α endonuclease specific inhibitor with cytotoxic activity against human multiple myeloma. *Blood* **117**, 1311–1314.
- 40 Han D, Lerner AG, Walle LV, Upton J-P, Xu W, Hagen A, Backes BJ, Oakes SA & Papa FR (2009) IRE1 α kinase activation modes control alternate endoribonuclease outputs to determine divergent cell fates. *Cell* **138**, 562–575.
- 41 Tsuru A, Imai Y, Saito M & Kohno K (2016) Novel mechanism of enhancing IRE1 α -XBP1 signalling via the PERK-ATF4 pathway. *Sci Rep* **6**, 24217.
- 42 Zhao N, Cao J, Xu L, Tang Q, Dobrolecki LE, Lv X, Talukdar M, Lu Y, Wang X & Hu DZ (2018) Pharmacological targeting of MYC-regulated IRE1/XBP1 pathway suppresses MYC-driven breast cancer. *J Clin Invest* **128**, 1283–1299.
- 43 Casper M, Weber SN, Kloor M, Müllenbach R, Grobholz R, Lammert F & Zimmer V (2013) Hepatocellular carcinoma as extracolonic manifestation of Lynch syndrome indicates SEC63 as potential target gene in hepatocarcinogenesis. *Scand J Gastroenterol* **48**, 344–351.
- 44 Fritz JM & Weaver TE (2014) The BiP cochaperone ERdj4 is required for B cell development and function. *PLoS ONE* **9**, e107473.
- 45 Shaffer A, Shapiro-Shelef M, Iwakoshi NN, Lee A-H, Qian S-B, Zhao H, Yu X, Yang L, Tan BK & Rosenwald A (2004) XBP1, downstream of Blimp-1, expands the secretory apparatus and other organelles, and increases protein synthesis in plasma cell differentiation. *Immunity* **21**, 81–93.
- 46 Pramanik J, Chen X, Kar G, Gomes T, Henriksson J, Miao Z, Natarajan K, McKenzie AN, Mahata B &

- 1 Teichmann SA (2017) The IRE1a-XBP1 pathway
2 promotes T helper cell differentiation by resolving
3 secretory stress and accelerating proliferation. *bioRxiv*,
4 235010 [PREPRINT].
- 5 47 Chaudhari N, Talwar P, Lefebvre D'hellencourt C &
6 Ravanan P (2017) CDDO and ATRA instigate
7 differentiation of IMR32 human neuroblastoma cells.
8 *Front Mol Neurosci* **10**, 310.
- 9 48 Sato F, Matsukawa Y, Matsumoto K, Nishino H &
10 Sakai T (1994) Apigenin induces morphological
11 differentiation and G2-M arrest in rat neuronal cells.
12 *Biochem Biophys Res Commun* **204**, 578–584.
- 13 49 Brown A, Jolly P & Wei H (1998) Genistein modulates
14 neuroblastoma cell proliferation and differentiation
15 through induction of apoptosis and regulation of
16 tyrosine kinase activity and N-myc expression.
17 *Carcinogenesis* **19**, 991–997.
- 18 50 Matthay KK, Reynolds CP, Seeger RC, Shimada H,
19 Adkins ES, Haas-Kogan D, Gerbing RB, London WB
20 & Villablanca JG (2009) Long-term results for children
21 with high-risk neuroblastoma treated on a randomized
22 trial of myeloablative therapy followed by 13-cis-
23 retinoic acid: a children's oncology group study. *J Clin*
24 *Oncol* **27**, 1007.
- 25 51 Mérot Y, Ferrière F, Debroas E, Flouriot G, Duval D
26 & Saligaut C (2005) Estrogen receptor alpha mediates
27 neuronal differentiation and neuroprotection in PC12
28 cells: critical role of the A/B domain of the receptor. *J*
29 *Mol Endocrinol* **35**, 257–267.
- 30 52 Niederreiter L, Fritz TM, Adolph TE, Krismer AM,
31 Offner FA, Tschurtschenthaler M, Flak MB, Hosomi
32 S, Tomczak MF, Kaneider NC *et al.* (2013) ER stress
33 transcription factor Xbp1 suppresses intestinal
34 tumorigenesis and directs intestinal stem cells. *J Exp*
35 *Med* **210**, 2041–2056.
- 36 53 Wu PY, Liao YF, Juan HF, Huang HC, Wang BJ, Lu
37 YL, Yu IS, Shih YY, Jeng YM, Hsu WM *et al.* (2014)
38 Aryl hydrocarbon receptor downregulates MYCN
39 expression and promotes cell differentiation of
40 neuroblastoma. *PLoS ONE* **9**, e88795.
- 41 54 Monaghan TK, Mackenzie CJ, Plevin R & Lutz EM
42 (2008) PACAP-38 induces neuronal differentiation of
43 human SH-SY5Y neuroblastoma cells via cAMP-
44 mediated activation of ERK and p38 MAP kinases. *J*
45 *Neurochem* **104**, 74–88.
- 46 55 Ravanan P, Sano R, Talwar P, Ogasawara S,
47 Matsuzawa S-I, Cuddy M, Singh SK, Rao GS,
48 Kondaiah P & Reed JC (2011) Synthetic triterpenoid
49 cyano enone of methyl boswellate activates intrinsic,
50 extrinsic, and endoplasmic reticulum stress cell death
51 pathways in tumor cell lines. *Mol Cancer Ther* **10**,
52 1635–1643.
- 53